Evidencing risk to inform best practice: the limitations of detecting tinning layers by visual analysis during the removal of corrosion from archaeological iron

David E. Watkinson[a*], Michelle Crepeau[a] and Nicola J. Emmerson[a]

[a] School of History, Archaeology and Religion, Cardiff University, John Percival Building, Colum Drive, Cardiff CF10 3EU, UK

***Author for correspondence**

Abstract

Evidence for tinning on corroded archaeological iron is visible in X-radiographs as distinct thin high density white lines. These are used to guide the removal of overlying iron corrosion to reveal the tin layer. Airbrasion with 53µm aluminium oxide, at low pressure and powder flow, was used to remove iron corrosion incrementally from a tinned medieval key. Appearance of the tin layer visible on the radiograph was aided by optical microscopy. At selected points during the cleaning, SEM-BEI imaging with EDA spot analysis was used to determine if the tinning layer had been reached. Comparing optical assessment with SEM-BEI images revealed that the occurrence of tinning could not be detected with the naked eye aided by optical microscopy. No metallic tin was observed and it is presumed to be present as tin dioxide (SnO_2). The presence of tinning was confirmed by SEM-EDA spot analysis. It is likely that parts of the tinning layer were lost during airbrasion. This identifies the risk of removing overlying iron corrosion products to expose tinning layers. Conservation strategies for preserving tinning layers on iron need to be formulated according to evidence that tinning cannot be readily detected by optical microscopy and elemental surface analysis is required to confirm its presence.

Keywords: iron; tinning; archaeological; corrosion; airbrasion; radiography; SEM-BEI

1. Introduction

1.1 Context for study

Dissimilar metal coatings such as silver, tin and copper have been applied historically to iron to decorate and/or protect objects (Oddy 1980; Corfield 1985; Meeks 1993). Construction methods such as brazing may also leave thin coatings of metal on iron. On archaeological iron, these coatings are normally obscured by overlying corrosion products and it is radiography that alerts the conservator to their presence. The qualitative nature of radiography means the layers are identified by the position, density and thickness of lines on the X-ray plate. Potential misidentification of layers as dissimilar coatings, when they are in fact dense corrosion product layers, can occur. Visual non-detection of tinning layers during removal of overlying iron corrosion is often attributed to such misidentification but the question remains whether the layer was missed by the conservator during cleaning. Expectation is that a shiny, silver coloured layer or a grey tin dioxide (SnO_2) layer will be

revealed. No study has attempted to align incrementally what is visible on the object during cleaning with semi-quantitative analysis of the surface, which would establish how easy it is to detect the layers relative to their presence as metallic tin or its oxide. Insight into how difficult this can be will inform best practice on cleaning iron objects thought to have tinning layers and identify the relative risk associated with the cleaning process.

1.2. Tinning in antiquity

Application of tin coatings to copper alloys is mentioned in the writings of Pliny the elder in his *Naturalis Historiae* but there is there is no parallel recording of tinning of iron. It has been reported as occurring in Europe from 500BC and from 5th century AD in Britain (Meeks 1993). Fusion plating of tin to wrought iron involves the application of heat to create an intermetallic phase with iron, which binds it to the metal surface (Meeks 1993; Dionisio 1985). Tinning applied by wiping involves the use of rosin as a flux to clean the iron, followed by the application of tin or tin/lead solder filings which are melted by heat and wiped over the surface. Hot dipping in a heated liquid tin bath is also a technique that can be employed. The low solubility of tin in other metals means a very thin intermetallic layer (<1µm) comprising two intermetallic phases occurs; FeSn (η = 68%Sn) and the predominant thermodynamically stable phase $FeSn_2$ (θ = 81%Sn) (Dionisio 1985). The excess layer of metallic tin will sit on top of this thin intermetallic phase. Adhesion to the metal can be improved by scoring of the metal to key the tin onto the surface.

1.3. Corrosion of tin layers on wrought iron

The electrode potential of tin (-0.136V) makes it cathodic to iron (-0.44V), consequently it might be expected to survive in burial contexts sandwiched between iron corrosion products. However, once isolated in this way, it can corrode (provided there is oxygen and moisture access to it) with grey/white SnO_2 as the thermodynamically favoured product (Turgoose 1985). Since SnO_2 is highly insoluble, except in strong acids and alkalis, it is immobile and is expected to remain in its original position on the object. Studies of corrosion on archaeological bronzes show that this occurs within the alloy and it is a marker layer for original surface on these objects (Piccardo and Robbiola 2007). Consequently, oxidised tinning layers are expected to provide clear markers for the original surface on an archaeological iron object. Lead (mp 327.5^{o}C) may be mixed with tin (mp 231.7^{o}C) to produce tinning layers. Its electrode potential (-0.126V) is close enough to that of tin for each metal to corrode independently when mixed together (Turgoose 1985). Although these lead compounds are more soluble than SnO_2, a dense corrosion product layer is expected to occur because of the immobility of tin. This is readily detectable by X-radiography, as the atomic weights of tin (118.7) and lead (208.2) greatly exceed that of iron (56). Corrosion products on archaeological iron have been characterised extensively (Neff et al. 2007). If the tinning does not migrate from its original position during corrosion, it will sit on the dense corrosion product layer (DPL) (Bertholon 2001) and will be overlaid with the transformed corrosion matrix (TM) that incorporates soil particles within it and is normally

less dense, more porous and softer than the DPL. The DPL likely comprises mostly α-FeOOH, Fe_3O_4 and γ-Fe_2O_3, while the altered layer will mostly be α-FeOOH but can contain many other iron corrosion products. The DPL is normally grey/black due to the Fe_3O_4 distributed within it.

1.4. Radiography of iron and airbrasion of corrosion products to expose tinning layers

X-radiography is commonly used to examine all iron from archaeological excavations to determine its shape, assess its condition, detect decoration and identify technological processes used in its manufacture. It is a qualitative technique that relies on the knowledge and skill of the operator to detect features in objects. A tungsten filament is heated to emit electrons and these are accelerated by a voltage (KV) then collide with a tungsten target causing emission of X-rays capable of passing through matter. These are collimated to strike an object that sits on either a photographic plate or X-ray sensitive detector surface, which darkens according to the number of X-rays that strike it. Differential adsorption and filtering of the X-rays occurs within the object according to their wavelength and the density and thickness of materials that comprise the object. A dense white or light grey line will be produced by tinning or other layers isolated from the iron surface by corrosion products, provided their atomic weight significantly exceeds that of metallic iron and its corrosion products. Misidentification may occur if thin white lines produced by very dense corrosion product layers formed at the metal surface are present. Since these are often thicker and less intense than tinning, the skill of the conservator is essential for the identification process. Where tinning has been lost from a surface, traces frequently survive in corners and undercuts where it has pooled into a thicker layer during its application to the object.

An oft-used procedure for revealing dissimilar metal layers, or the marker layer of corrosion representing the original surface of an iron object, is removal of overlying corrosion products using an airbrasive machine, which has been shown to be a very sensitive and controllable tool (Farooq 2011). This technique normally utilises small particles of aluminium oxide expelled under pressure from a nozzle to cut the corrosion product from the object surface. Detection of the tinning layer relies upon the machine operator referencing the radiograph of the object while using a microscope during the airbrasion process and their expertise to visually detect the layer as it appears. With such thin layers this can be challenging, even when they retain metallic tin; when they exist as corrosion products it is exceptionally difficult, as the SnO_2 is similar in colour to the α-FeOOH/Fe_3O_4/γ-Fe_2O_3 DPL matrix that would normally underpin it. It would be easy to simply remove the SnO_2 layer without detecting a colour change. Morphologically, there is little information on the nature of the SnO_2 layer that might aid in its detection. It might be expected to be softer and less coherent than an iron corrosion matrix containing dense Fe_3O_4 but infusion of dense iron corrosion products such as Fe_3O_4 into the layer could contribute to improved hardness. Currently, there is no research available to identify whether a SnO_2 layer is infused with iron corrosion, nor is there data on its hardness and colour.

1.5 Experimental aims and objectives

Aim:

- To provide an evidence based assessment of the effectiveness of visual inspection as a method for detecting the presence of tinning layers on archaeological iron objects.

Objectives:

- Use radiography to tentatively identify tinning layers on a medieval key.
- Remove overlying corrosion products incrementally by airbrasion and record the surface as cleaning progresses using visual inspection, microphotography, SEM-BEI imaging and SEM-EDX spot analysis to detect elemental composition.
- Compare the results from visual interpretation to those from elemental composition.
- Assess the degree of certainty attached to using visual inspection for determining end point when removing corrosion products overlying tinning layers.

2. Method

2.1 Sample selection

The sample is a late (14^{th}-15^{th} C) Medieval key from the deserted Medieval village at West Whelpington, Northumberland, UK (Evans and Jarrett 1987). Radiography (Faxitron 438505 110KV) reveals it to have a tubular shaft, designed to accept the guide pin in a lock, with extensive mineralisation evidenced by the low overall density of the bow, tube walls and ward (Figure 1). Lamellar structures in the bow evidence slag planes from forging. There are multiple areas where a dissimilar metal (henceforth referred to as tinning) is present as a coating and potentially as decoration in incised areas of the key. The tinning is covered by a thick corrosion product layer and records reveal that the key had already been subjected to some mechanical cleaning. This revealed its general shape but failed to show any evidence of the tinning visible in the radiograph.

The site had been published and permission had been obtained for destructive investigation. The ethical rationale behind this decision is clear, information gained from this study can be used to guide protocol for the mechanical cleaning of similar objects. Improved understanding of the relationship between corrosion processes, radiographic imaging and visual detection of dissimilar metals will contribute to devising corrosion removal strategies and limit loss of evidence. It will also inform decision making regarding whether to clean objects or to use only radiographs for interpretation and publication, due to the level of risk associated with their loss during cleaning.

Figure 1. *Medieval key from West Whelpington deserted Medieval village before airbrasion and radiograph showing hollow barrel construction with tinning residues. Areas 1-6 selected for airbrasion to expose tinning layers. Dotted line for area 6 indicates it is an edge, as the ward was broken at that point and removed to reveal a cross section.*

2.2 Investigative method

Using a Faxitron 43805 X-ray machine, side and dorsal radiographs of the key were taken at 30 second intervals over a 5 minute period at 95, 100 and 105KV to fully determine location of the tinning (Figure 2). Results identified optimum exposure values for KV and time to record the tinning (90 kV; 3 minutes; 3 Ma constant) and informed selection of 6 areas where there was tinning and where the key would be mechanically cleaned (Figure 1). This employed a Texas Airsonics AJ-1™ spirofeed airbrasive machine to deliver 53µm diameter aluminium oxide particles at pressures ranging from 20-60 psi at powder flow level 4 (full scale 1-10). The powder was fed at a working distance of 2-6mm and an angle of 45^{o} for optimum effect (Farooq 2011) and the operator used a x10 stereo microscope to view the object during the cleaning process. Post-airbrasion the key was washed in baths of benzyl alcohol to remove aluminium oxide particles lodged on the surface of the key, as their presence reflects light that mimics the appearance of a metallic coating under the microscope. Removal of iron corrosion was subjective, mimicking real practice. Its progress

was determined at selected intervals by inspection and recording using unaided visual inspection, radiography, photomicroscopy, scanning electron microscopy (SEM) and energy dispersive X-ray analysis (EDA).

Radiography used the optimum parameters identified in the radiography calibration previously described. Stereomicroscopy, over a magnification range x4 to x40, was carried out using a Nikon SMZ1000 equipped with a Nikon Coolpix 4500™ camera supported by NIS Element D 3.0™ software to digitally record images. SEM employed a CamScan 2040 SEM with Oxford Link Pentafet 5518 dispersive X-ray spectrometer and Maxim™ imaging and INCA analysis software packages. Backscattered electron imaging mode (BEI) was used to image cleaned areas and spot analysis with EDA determined elemental composition at the surface. Since higher atomic weight elements produce greater contrast, tin or SnO_2 would be visible against the iron oxides around them. The use of carbon coating for SEM imaging was avoided by use of EnVac mode with a 20keV beam current. Although carbon coating increases conduction, lessens charge and improves image quality, its use would have been problematic since it would have to be removed before recommencing airbrasion. The data was ZAF corrected and normalised. No calibration standard was used but acquisition rates and dead time were maintained at 3000 and 20-50 respectively. Since the SEM was employed in spot analysis mode as a detection tool for presence or absence of tinning, the 1-10 wt% detection was acceptable. The SEM detects elements rather than compounds, so any confirmation that the tin was still metallic was determined by stereomicroscopy. EDA spot analysis of tinning sites was guided by the BEI images.

3. Results

The key is extensively mineralised, particularly in the areas of the bow and ward (Figure 2). It retains radiographic evidence of a dissimilar metal within its construction, as a coating and within incised lines. The bit has thick layers of dissimilar metal in right angled areas where the coating has pooled during its application. There are also incised cuts visible, particularly on the tooth closest to the main body of the shaft. These may be deliberate additions to aid keying onto the surface of the iron. The dense, hard outer corrosion layer has been smoothed by previous mechanical cleaning carried out in the 1970s. The appearance of its surface suggests that a rotary grinding wheel has been used in this process (Figure 1). The use of a ‘mini-drill’ with rotary burrs was a popular and acceptable method for removing corrosion in the past, normally prior to the use of the more sensitive airbrasion technique to reveal detail, which does not appear to have been carried out. The abrasion technique employed in this study effectively cut ‘trenches’ into the corrosion layers in search of the tinning (Figures 3,6). In figure 4 BEI images and EDA analysis of selected areas of the key confirm the layer seen on the X-radiograph is tinning. Visual evidence of tinning is recorded in figures 5-7, accompanied by BEI imaging to confirm the presence of tinning layers and X-radiographs to identify the guidance used to guide airbrasion.

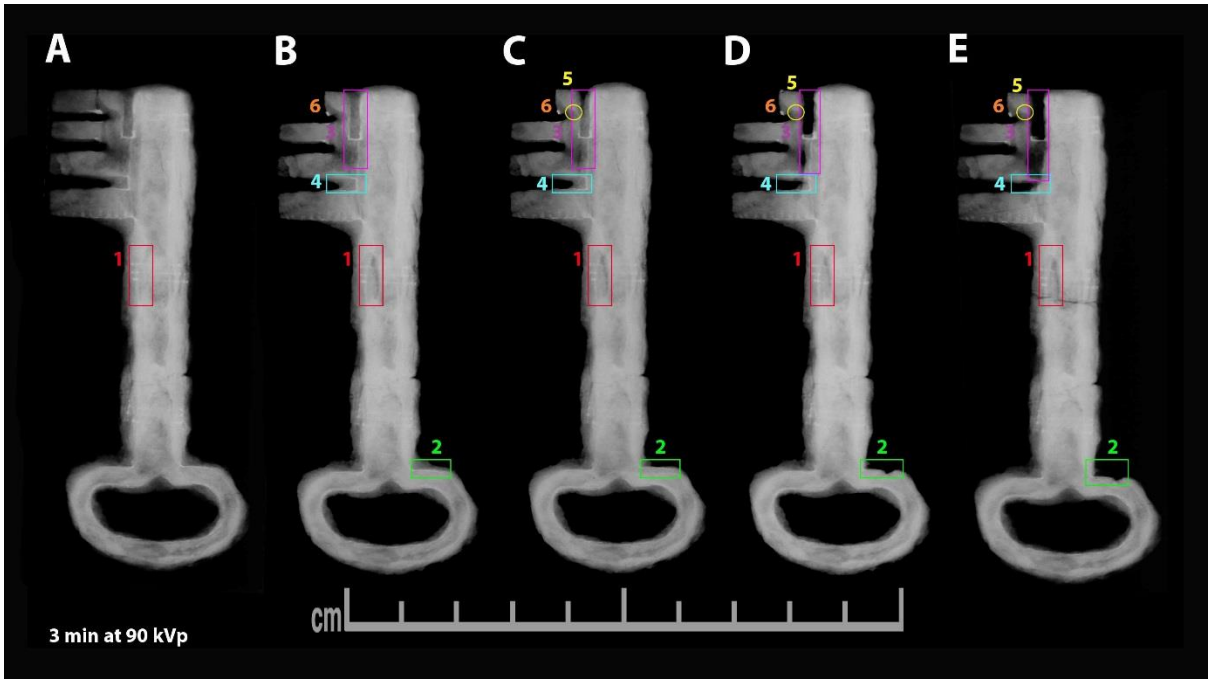

Figure 2. *Radiographs of key ventral and left profile at 110, 100, 95 and 85 kV 5 minute exposure.*

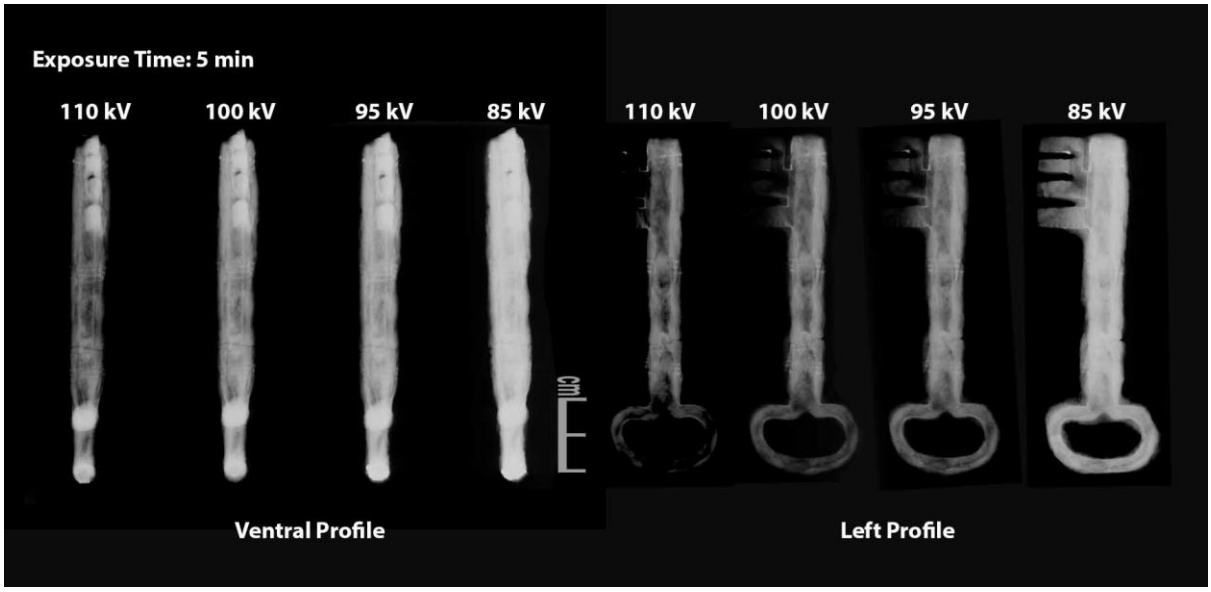

Figure 3. *Radiographs recording incremental removal of iron corrosion by airbrasion in designated investigation areas 1–6 (Figure 1). Radiograph A records the key before airbrasion, with the broken end ward in place. Images B to E record progressively the removal of corrosion overlying the suspected tinning areas.*

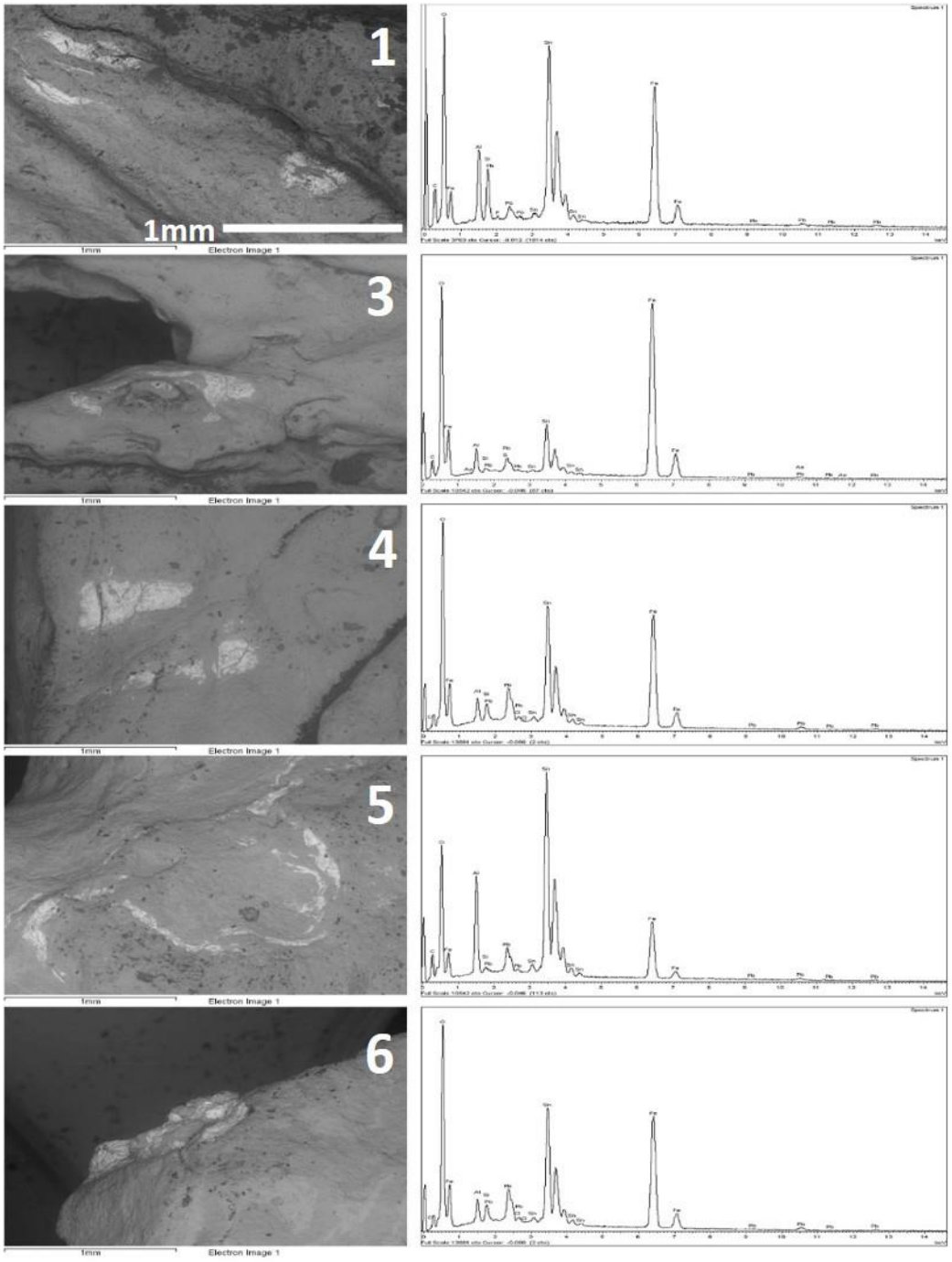

Insert

Figure 4. *SEM-BEI images and EDA spectra of tinning in areas 1, 3, 4, 5 and 6 (see Figure 3) following completion of airbrasion. All images are recorded at the same magnification (1mm scale in image 1)*

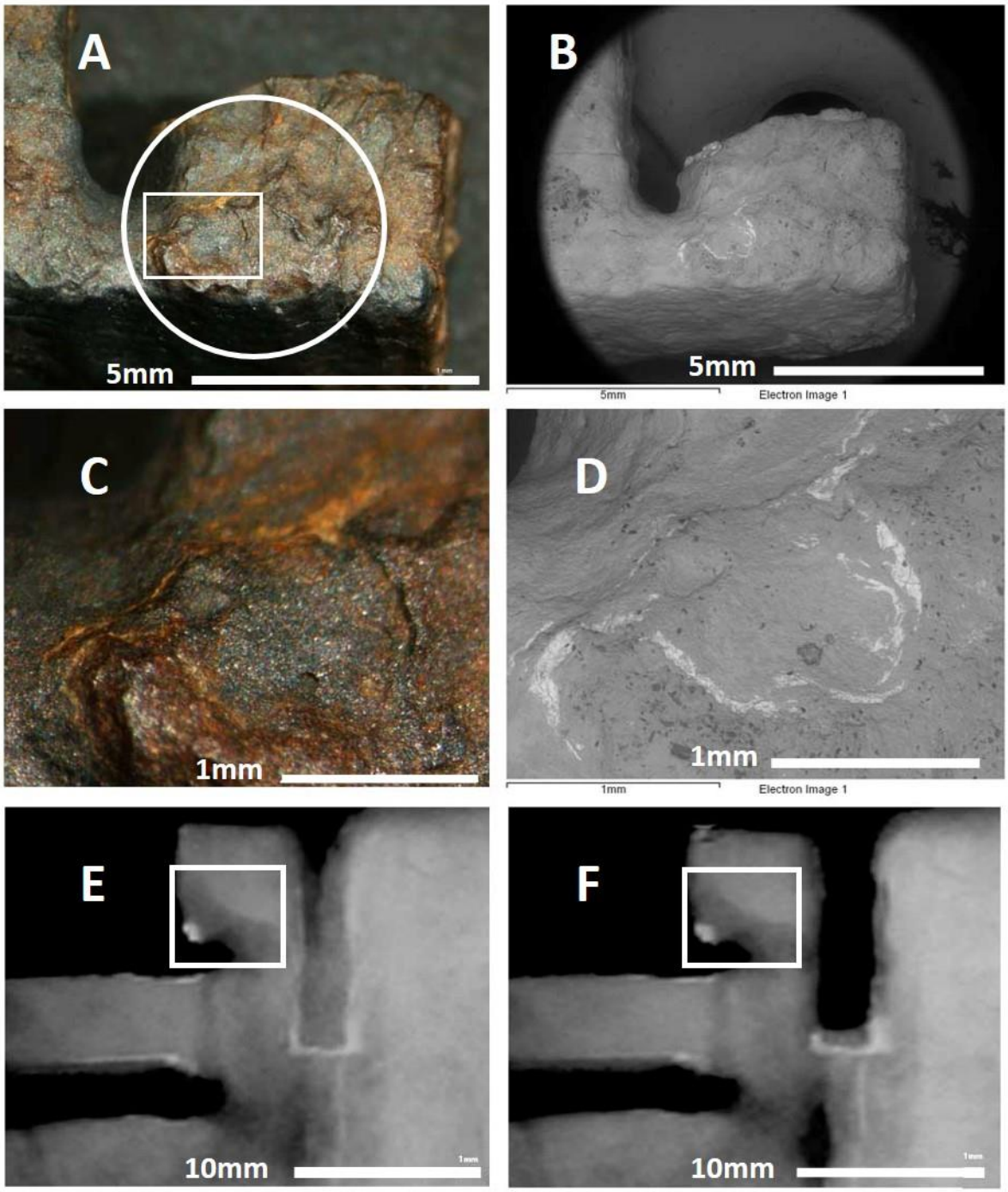

Figure 5. *Optical microscopy, SEM-BEI images and radiographs of site 5, flat face of broken ward on the key bit. Image A; optical microscopy image where the circle delineates area 5 post-airbrasion and the rectangle identifies area recorded in optical microscopy image C and BEI image D. Image B is a BEI image of the ward. The rectangle within the radiograph in image E identifies in detail area 5 as it appeared before airbrasion and F records it after airbrasion; no evidence of tinning on the face of ward is visible either before or after airbrasion.*

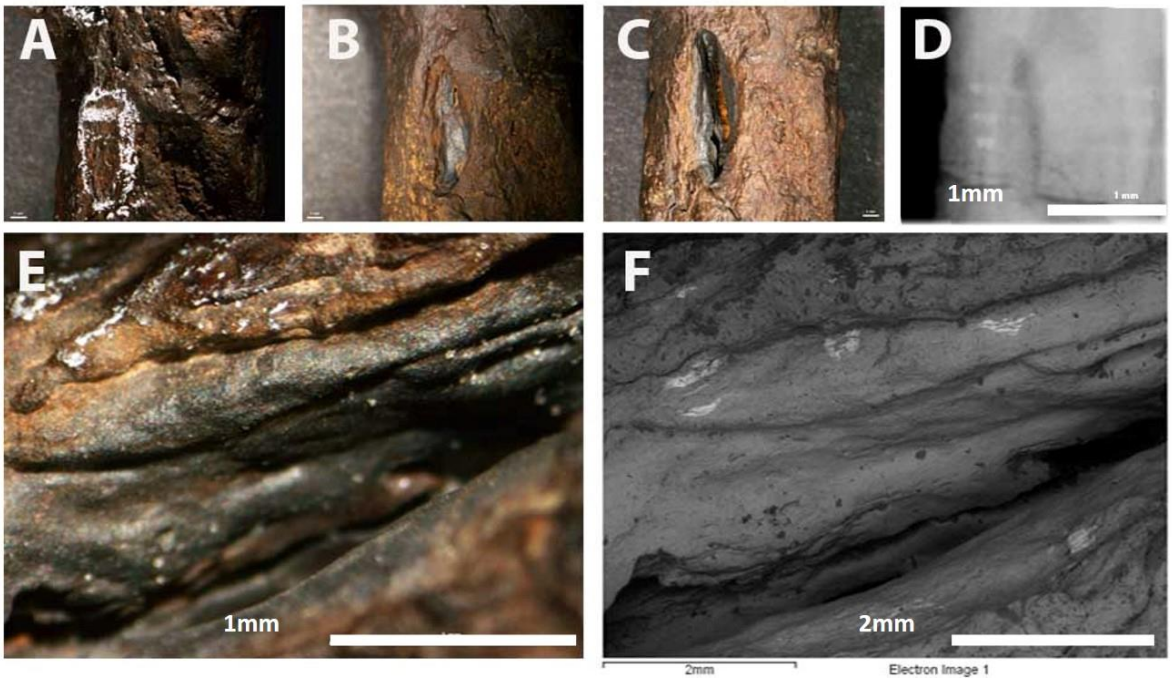

Figure 6. *Optical microscopy, SEM-BEI images and radiographs of site 1; decorative lines on the shaft. Image A is the area to be airbraided marked in china pencil. Images B and C record progress of airbrasion. Image D is a radiograph of site 1 post-airbrasion showing tinning lines have been lost during removal of corrosion. Image E confirms the remains of the 3 tinning lines visible in the BEI image E is undetectable using optical microscopy.*

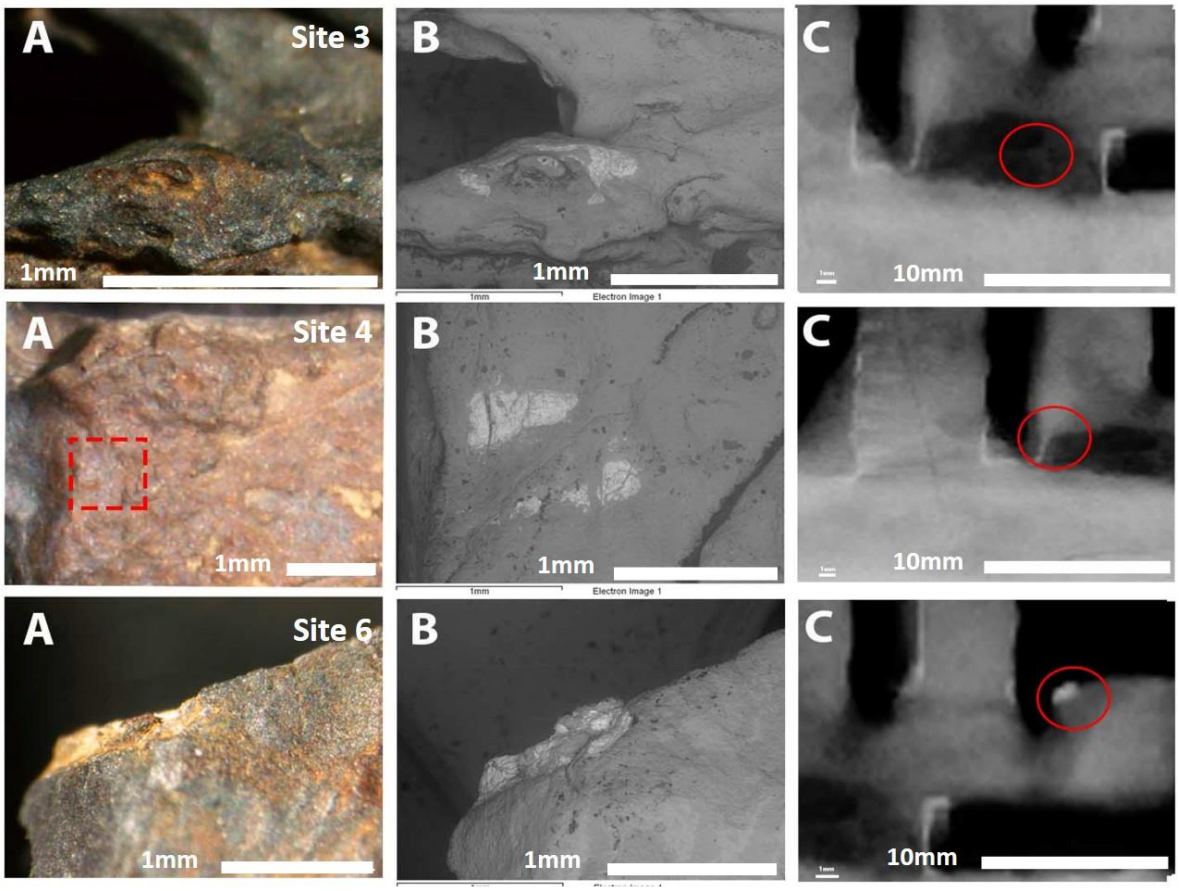

Figure 7. *Optical microscopy (A), SEM-BEI images (B) and radiographs (C) of site 3 (shaft) and sites 4 and 5 (ward) following airbrasion.*

Discussion

Although airbrasion was carried out with the aid of a microscope, guided by radiographs and using low pressure and powder feed for controlled corrosion removal, identifying an end point that exposed tinning layers was difficult as no tinning was seen by eye during this process, either as a shiny silver-coloured metal or a grey oxide. Subtle differences between a grey SnO_2 layer and the iron corrosion products in the DPL and TM would be difficult to observe, especially if the SnO_2 contains iron corrosion within its matrix. There is no data published identifying the morphology and metallic/compound composition of SnO_2 layers on corroded iron objects, which would aid identification.

Even when using optical microscopy guided by SEM-BEI images, it was not possible to detect the tinning visible on the SEM-BEI images and elementally confirmed by EDA spot analysis (Figure 4). The tinned areas are discontinuous and very small (<1 mm), although more tinning may lie undetected below overlying iron corrosion, alternatively the gaps in continuity may be because tinning was inadvertently lost during airbrasion. The thinness of tinning layers makes it easy to pass through them during airbrasion, even if they are readily detectable by eye. Spot analysis detected the presence of small amounts of lead in all the tinning layers.

Comparing SEM-BEI and optical microscopy images, it is clear that the tinned areas are undetectable by eye, despite the aid of a microscope (figures 5-7). Figure 5 records the flat face of the ward that is area 5 on the key and while tin is detected in BEI images (5B,C), no metallic tin is visible post-airbrasion (5A,C) and the SnO_2 present cannot be differentiated from the iron corrosion. Radiographs (5E,F) do not show the tinning as a distinct line to guide the conservator during airbrasion, since they are taken at 90^o to its surface recording its thinnest point. In contrast, dense white lines occur at object edges because their thickness is effectively increased by the depth of the object. In Figure 6, the three distinct tinning lines on the shaft (area 1; 6D) are marked out with grease pencil (6A) for airbrasion (6B,C,E). The three lines are invisible to the eye in the airbraded area but traces of them are detected in BEI (6F), where it appears that airbrasion had inadvertently cut through them without this being detected by eye during removal of iron corrosion. Invisibility to the eye while being detected by BEI is repeated for tinning layers across the object (Figure 7).

The study reveals the difficulty of identifying tinning by visual means as an object is cleaned. The radiographs were highly informative, yet the tinning was impossible to see with the aid of optical microscopy. For some samples, two conservators with 40 years of experience between them and a student could not detect evidence of tinning using optical microscopy. Even with the aid of a BEI image to confirm the location of the tinning, it was rare that observers could actually identify colour or morphological differences that differentiated the areas of tinning from the general surface of the object. A second publication based on this key will report morphology and composition of the corroded tinning layers.

Conclusion

Evidence from this study indicates that using airbrasion to reveal tinning layers on archaeological iron, guided by radiography and optical microscopy, is a high risk exercise. Without tinning surviving in a metallic state, its visual detection was not possible. It is almost certain that evidence for tinning will be lost during removal of iron corrosion because evidence of its presence cannot be seen and the layers are thin. SEM-BEI imaging can be used to detect tin and confirm technological processes but its use does not remove the risk of tinning loss during cleaning. Management discussions should include consideration about whether attempts to reveal tinning layers should be part of the conservation plan. Localised cleaning and SEM-BEI spot analysis to confirm the presence of tin for reporting purposes will be a less destructive approach, leaving the remainder of the object uncleaned for future reference.

Acknowledgements

Thanks to Dr David Evans for releasing the West Whelpington key for research purposes.

References

Bertholon, R. 2001. Characterisation and location of the original surface of corroded archaeological objects. *Surface Engineering* **17**(3): 241 – 245.

Corfield, M.1985. Tinned iron. In: G. Miles and S. Pollard (Eds) *Lead Tin and Pewter* United Kingdom Institute for Conservation Occasional Paper No. **3**: 40-43.

Dionisio, P. H., de Barros, Jr. B. A. S. and Baumvol, I. J. R. 1985. Comparative study of intermetallic phases formed by direct ion implementation and radiation enhanced diffusion of tin in two kinds of steel. *Journal of Applied Physics* **58**(2): 773-778.

Evans, D. H. and Jarrett, M. G. 1987. The deserted medieval village of West Whelpington, Northumberland, third report, part one. *Archaeologia Aeliana* 5th Series **16**: 199-308.

Farooq, I., Imran, Z. and Farooq, U. 2011. Air Abrasion: Truly minimally invasive technique. *International Journal of Prosthodontics and Restorative Dentistry* **1**(2): 105-107.

Neff, D., Vega, E., Dillmann, P. and Descotes, M. 2007. Contribution of iron archaeological artefacts to the estimation of average corrosion rates and the long term corrosion mechanisms of low carbon steel. In: P. Dillmann, G. Beranger, P. Piccardo and H. Mathiesen (Eds) *Corrosion of Metallic Heritage Artefacts: Investigation, Conservation and Prediction of Long-term Behaviour*. Woodhead: Cambridge, U.K. 41-74.

Oddy, A. 1980. Gilding and tinning in Anglo-Saxon England. In: W. A. Oddy. (Ed) *Aspects of early metallurgy* British Museum Occasional Paper **17**. British Museum: London. 129-134.

Piccardo P., Mille, B. and Robbiola, L. 2007. Tin and copper oxides in corroded archaeological bronzes. In: P. Dillmann, G. Beranger, P. Piccardo and H. Mathiesen (Eds) *Corrosion of Metallic Heritage Artefacts: Investigation, Conservation and Prediction of Long-term Behaviour*. Woodhead: Cambridge, U.K. 239-62.

Turgoose, S. 1985. Corrosion of lead and tin: before and after excavation. In: G. Miles and S. Pollard (Eds) *Lead Tin and Pewter* United Kingdom Institute for Conservation Occasional Paper No. **3**. 15-26.